Sensors and Materials, Vol. 11, No. 4 (1999) 219–232
MYU Tokyo

S & M 0367

Six-Beam Twin-Mass Structure for Triaxial Accelerometer

José Antonio Plaza, Jaume Esteve and Emilio Lora-Tamayo

National Centre of Microelectronics (CNM) CSIC
Campus UAB 08193 Bellaterra, Spain

(Received April 27, 1998; accepted May 25, 1999)

Key words: silicon, triaxial accelerometer, piezoresistive

An open loop piezoresistive triaxial accelerometer with theoretically null cross-sensitivity has been designed, fabricated and characterized. The design is a twin mass structure with four lateral beams parallel to the masses in order to reduce the stresses induced by packaging and two central beams to avoid the yaw of the masses. Due to the complexity of its geometry, it was designed using the finite element method (FEM). The accelerometer has been fabricated and tested. The experimental sensitivities are 0.160 mV/(V·g) for the x direction, 0.093 mV/(V·g) for the y direction and 0.464 mV/(V·g) for the z direction with a nonlinearity better than 0.58% FS. These results are very promising and they are in agreement with the values obtained using the FEM.

1. Introduction

The need to measure acceleration has been the motive for the large number of one-axis commercial accelerometers. In the last decades, several commercial accelerometers have been produced using silicon micromachining.[1,2] These accelerometers have the advantages of microelectronics devices: *e.g.* small size, low price and good performance. The most common sensing elements used in silicon accelerometers are capacitors or piezoresistors.

In some applications, the measurement of the acceleration vector in its three components is required. For example, in gesture recognitions the use of triaxial accelerometers is

recommended.[3] Some other applications of these triaxial accelerometers are navigation, handling of fragile goods and earthquake monitoring.

Normally, in order to measure the acceleration vector, three uniaxial accelerometers are used. These accelerometers must be positioned perpendicular to each other. Therefore, the mounting of these devices is complicated because small differences in the angle between two accelerometers could introduce errors in the determination of every component of the acceleration vector. The idea of the detection of the three components of acceleration using only one device[4–14] has several advantages. It avoids the precise assembly of the three different devices. Moreover, it can be smaller than systems with three uniaxial accelerometers and therefore cheaper to fabricate.

The piezoresistive effect in silicon is well known.[15] It has high sensitivity with good linearity. Typically, four silicon piezoresistors in a Wheatstone bridge configuration define the sensing element. In these cases, the output of the devices is linear with acceleration. There is a large number of accelerometers using this principle.[16–19]

The main requirements of a triaxial accelerometer are high sensitivity, good linearity and low level of cross-sensitivity. A piezoresistive triaxial accelerometer[20] with good sensitivity and linearity and a theoretically null cross-sensitivity is presented in this paper. Special aspects shown in this paper are: FEM results of the reduction of package stresses by the use of lateral external beams, FEM results of the increase of sensitivity and figure of merit of the devices with such beams, FEM results of the reduction of the yaw between the two masses using two central beams, a circuit to detect the three components of the acceleration with only two Wheatstone bridges and how to control the damping of the accelerometer.

2. Design

The structure is a combination between a Quad-beam accelerometer[16] and a Twin-mass accelerometer designed by M.H. Bao.[17,18] It consists of two twin masses joined together by two central beams and joined to the frame by four lateral beams (Fig. 1).

Normally, the geometry of the conventional accelerometers are quite easy, so, an analytical modeling is enough to study such devices. On the other hand, the finite element method (FEM) has become a powerful tool in the design of complex structures. The economic cost and the time-consuming design is reduced using the FEM. Therefore, due to the complexity of the presented triaxial structure, the device was designed using the FEM. This method allows a more precise analysis of the structures and allows parameters that are difficult to obtain with analytical modeling, such as cross-sensitivities or natural frequencies of the devices, to be obtained.

The main problems with the Twin-mass accelerometer, Fig. 2(a), are the concentration of unwanted package and fabrication stresses in the central beam. The piezoresistors that detect acceleration are situated on the central beam, and therefore, such stresses can affect the sensitivity and linearity of the device. In order to minimize this problem, we have adapted the structure and redesigned the external beams parallel to the masses, as can be seen in Fig. 2(b). The Twin-mass structure is very sensitive to the stresses in the x direction

which concentrate on the central beam. On the other hand, in the case of the structure with the lateral beams parallel to the masses, the effect due to the stress in the x direction is reduced on the central beam, and therefore, on the piezoresistors. The lateral beams absorb the stresses in the x direction. A reduction of more than one order of magnitude of the stress on the central beam is shown by the FEM simulations using ANSYS 5.3. The package and fabrication stresses in the y direction have no significant effect over the central beam because they are absorbed by the masses.

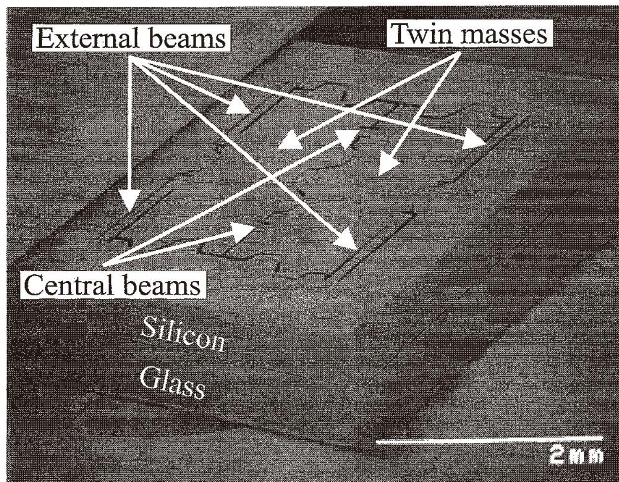

Fig. 1. SEM photograph of the triaxial accelerometer.

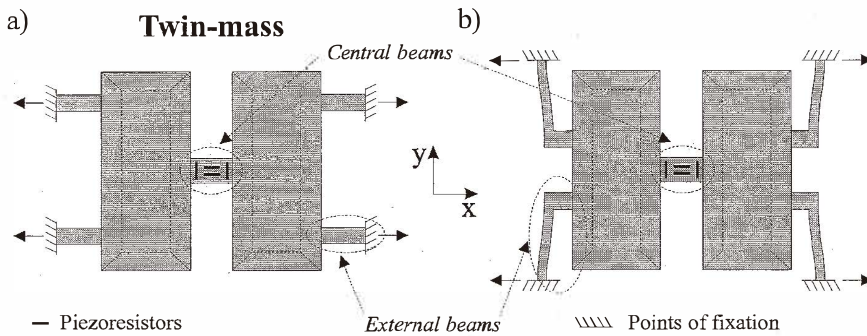

Fig. 2. (a) Twin-mass structure, (b) adapted Twin-mass structure with external beams parallel to the masses.

Another advantage of the lateral beams parallel to the masses is the increase in the sensitivity of the devices without any increase in the area of the chip (and therefore in its cost). The sensitivity of the device increases with the length of the lateral beams. In the standard Twin-mass structure, an increment in the length of the lateral beams means an increment in the area of the device. On the contrary, in the modified structure, the length of the lateral beams can be as long as half the side of the mass without any increase in the area of the chip. In Table 1, the characteristics of the two devices with different geometries are shown. The first one is a typical Twin-mass structure with 200 μm lateral beams. The second one has the same area but the external beams are parallel to the masses and their lengths are longer, 600 μm. The second device has a sensitivity 1.71 times higher than the first with only a reduction of 1.4 times in its natural frequency. This means that with the same area, both the sensitivity and the figure of merit of the second device are better.

In the Twin-mass design with parallel external beams, the stiffness in the x direction is very low so the masses can yaw, as can be seen in Fig. 3(a). We have designed a double central beam (Fig. 3.(b)) in order to avoid this problem. We have simulated using the FEM the yaw effect when there is only a single central beam and when there were two central beams (the width of the single central beam was twice the width of each of the double central beams). The simulation has shown that in the second case the yaw effect is reduced by a factor of 20 when the two beams are separated 1,000 μm (separation in the designed device). As an example, if the separation was 500 μm the reduction was only of a factor of 5.5. It can be observed that, increasing the distance between the two central beams, the yaw between the two masses decreases.

The final new structure consists of two twin masses of 3,020 $\times$ 1,420 μm^2 joined by two central beams and joined to the frame by four external beams parallel to the masses, Fig. 4. The dimensions of the central beams are 200 μm long by 150 μm wide and the dimensions of the external beams are 1,250 μm long by 150 μm wide. As well as the advantages already commented above, the new structure can also detect the three components of the acceleration vector.

Table 1
Comparison between standard Twin-mass structure and Twin-mass structure with lateral beams parallel to the masses. U_z: displacement perpendicular to the chip; S_l and S_t: stresses parallel and perpendicular, respectively, in the lateral beam where the piezoresistors are situated; Frec. N.: natural frequency of the devices.

	Twin-mass Perpendicular external beams (L_{beam} = 200 μm)	Twin-mass Parallel external beams (L_{beam} = 600 μm)
U_z [μm]	0.0844	0.162
S_l [MPa/g]	0.8430	1.4511
S_t [MPa/g]	0.0388	0.0580
Frec. N. [Hz]	2118	1508

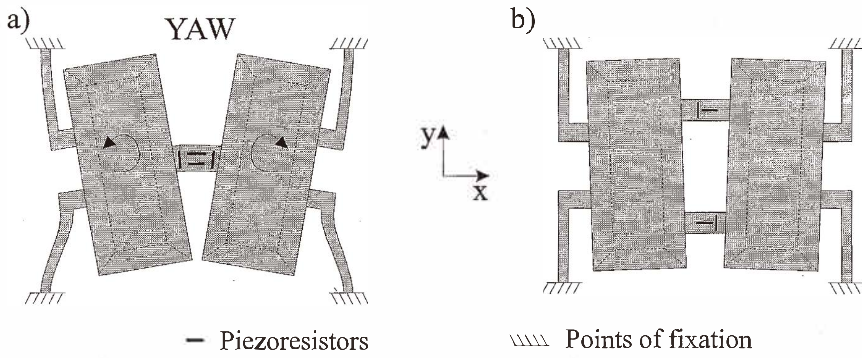

Fig. 3. Yaw of the masses with (a) one central beam and (b) two central beams.

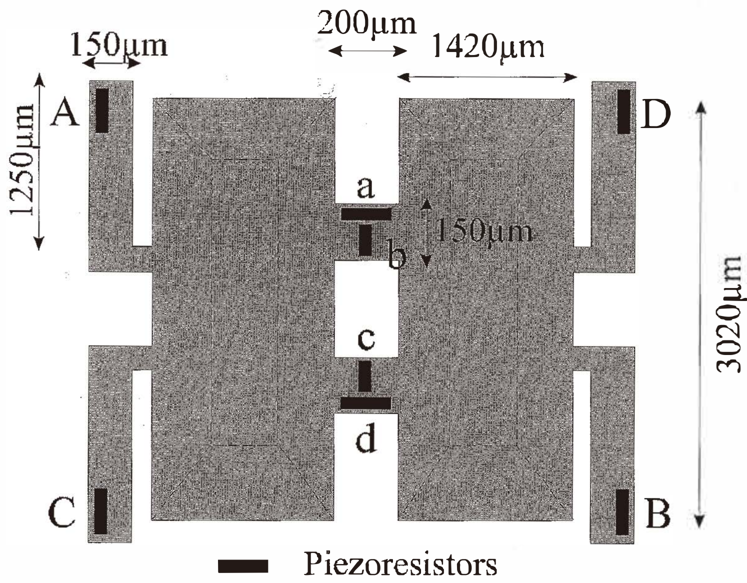

Fig. 4. Geometry and positions of the piezoresistors in the triaxial accelerometer.

3. Triaxial Detection

The new structure has been simulated by the finite-element method using ANSYS 5.3. The device displacement for z, y and x accelerations are shown in Fig. 5. The two twin masses move up when a negative z acceleration is applied, Fig. 5(a), in a similar manner as does the Twin-mass accelerometer.[17] Therefore, if a Wheatstone bridge of piezoresistors is defined in the central beams, it is possible to detect the z acceleration with null cross-sensitivity. When a y acceleration is applied, the two masses tilt around the x axis and therefore, two external beams move up and the opposite external beams move down, Fig. 5(b). Finally, when an x acceleration is applied to the device, one mass moves up and thus its external beams and the other mass and its external beams move down, Fig. 5(c).

The location of the piezoresistors in the device is shown in Fig. 4. Piezoresistors a, b, c, and d, located in the central beams, are used for the detection of z acceleration. Piezoresistors A, B, C and D, located in the external beams, are used for the detection of the y and x accelerations. The configuration of the piezoresistors forming the different Wheatstone bridges and the effect of the acceleration over the different piezoresistors are shown in Fig. 6. When z acceleration is applied, piezoresistors c and b increase their resistance and piezoresistors a and d decrease their resistance; therefore, Wheatstone bridge Z has an output linear with the z acceleration. When a y or x acceleration is applied to the device, the masses move in the same plane so the central beams are not stressed. Therefore, the output of Wheatstone bridge Z is null for x and y accelerations. In the case of y acceleration, piezoresistors A and D increase their resistance and B and C decrease their resistance. Wheatstone bridge Y is sensitive to y acceleration. If z acceleration is applied, the four piezoresistors, A, B, C and D, change identically and the output of Wheatstone bridge Y is zero. When x acceleration is applied, piezoresistors B and D increase their resistance and piezoresistors A and C decrease their resistance, and consequently, change of Wheatstone bridge Y is null. The effect is similar for Wheatstone bridge X, but in this case it is sensitive to x acceleration but not sensitive to y and z accelerations. Remember that the Y and X Wheatstone bridges are formed by the same piezoresistors A, B, C and D but with a different configuration.

The stress that affects the different piezoresistors (S_l longitudinal stress and S_t transversal stress), when 1 g accelerations in the three orthogonal directions are applied to the device, is shown in Table 2. Also shown is the sensitivity of each Wheatstone bridge to the different accelerations and the maximum z displacement for 1 g acceleration.

The first mode of vibration of the device is shown in Fig. 5(d). The deformation of the first mode is similar to the deformation when z acceleration is applied and the frequency is 679 Hz. The frequencies of the first three modes of vibration are shown in Table 3.

In order to detect the x and y accelerations, it is necessary to have two Wheatstone bridges with piezoresistors located in the external beams. The number of metal lines necessary to connect the three Wheatstone bridges, i.e. 12 piezoresistors, is very large. The metal lines of aluminium and the necessary oxide used to prevent short circuit between the aluminium and the bulk silicon introduce unwanted stresses to the beams. Another problem related to a large number of Wheatstone bridges in the devices is the connection between the different piezoresistors that form the three Wheatstone bridges. This connec-

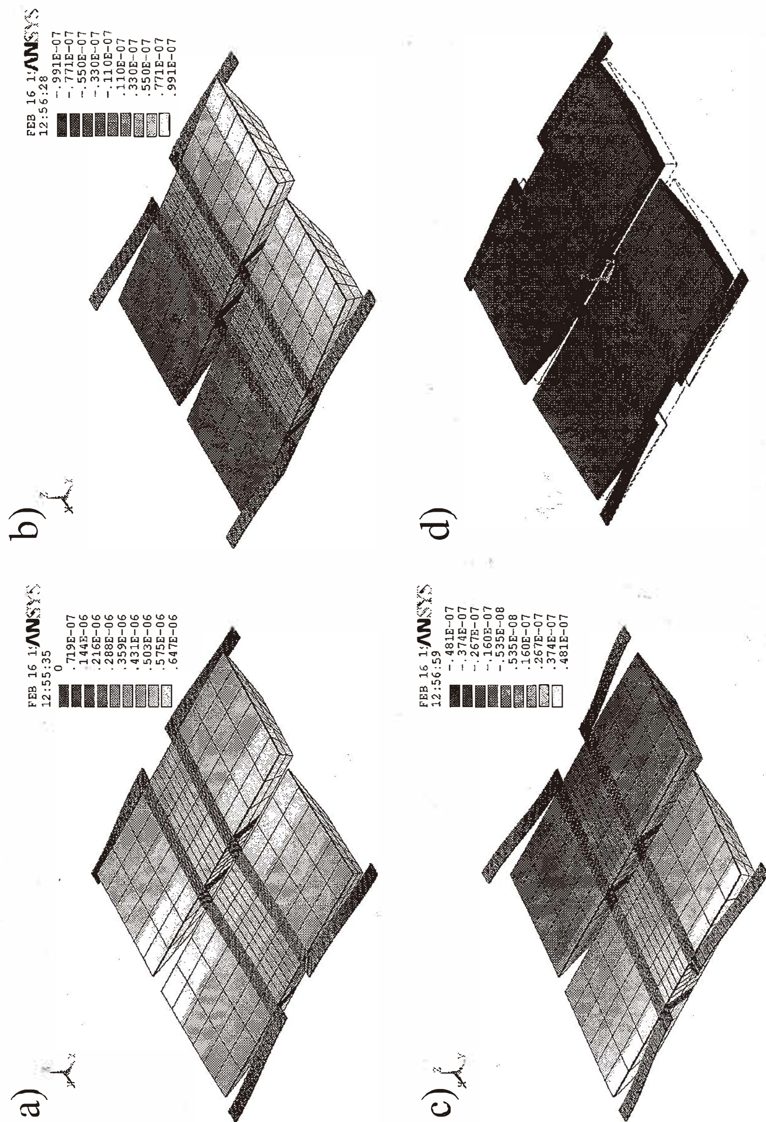

Fig. 5. FEM results. Displacement [m] of the accelerometer for 1 g (a) z acceleration, (b) y acceleration and (c) x acceleration. (d) Deformation of the first mode of vibration.

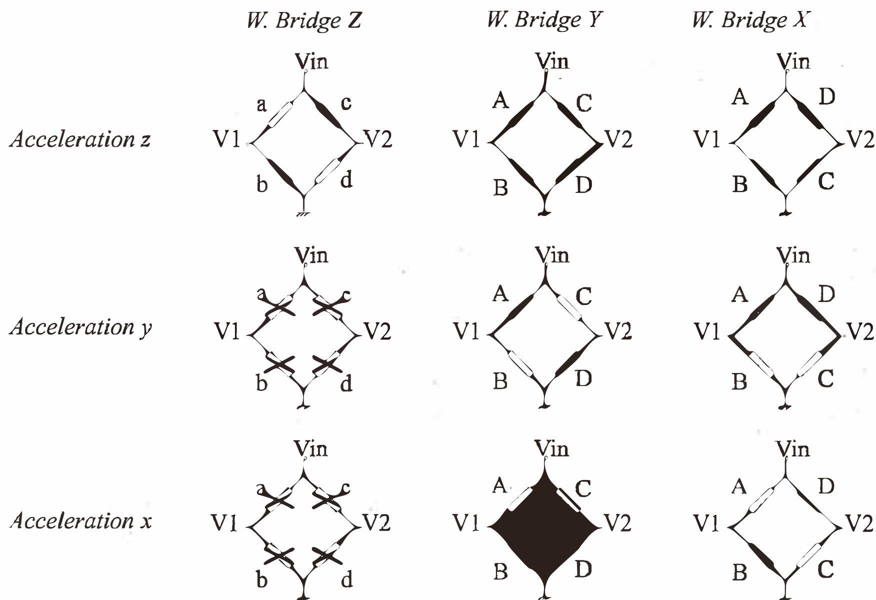

Fig. 6. Effect of acceleration on the piezoresistors. Black resistors increase their resistance, white resistors decrease their resistance and crossed ones do not change.

Table 2
Absolute stresses over the piezoresistors calculated using the finite element method. S_l and S_t: longitudinal and transverse stresses; sensi: sensitivity of the different Wheatstone bridges; z_{max}: maximum z displacement.

Acceleration	Piezo	S_l [MPa/g]	S_t [MPa/g]	sensi [mV/(V·g)]	z_{max} [μm/g]
x	A, B, C, D	0.308	0.087	0.159	0.048
y	A, B, C, D	0.192	0.00028	0.097	0.099
z	a, b, c, d	1.920	0.236	0.855	0.647

Table 3
Simulated frequencies of the first three modes.

	Mode 1	Mode 2	Mode 3
Frequency [Hz]	679	1016	1419

tion is not possible with only one metal layer.

We have reduced the number of piezoresistors to eight. Four piezoresistors in the central beams compose the Wheatstone bridge that detects z acceleration and the other four piezoresistors in the external beams are connected in pairs. The connections between the two pairs depend on the direction of the acceleration to be detected. With this configuration, the level of unwanted stress in the beams due to the metal lines and the number of interconnections is reduced. The other advantage is that, using only one metal layer, it is possible to make all the connections in the chip, except one. The reduction of three Wheatstone bridges to two is shown in Fig. 7.

It is possible to detect x and y accelerations at the same time if a square voltage is supplied (supply voltage, 0) to the $y_+ x_{off}$ terminal and a square voltage (0, supply voltage) to the $y_{off} x_+$ terminal. Therefore, the output $xy_{o1}\, xy_{o2}$ is a square signal where the first half of the period is the level of y acceleration and the second half is the level of x acceleration. We have developed and fabricated a circuit that apply a square signal to the $y_+ x_{off}$ and y_{off} x_+ terminals. The circuit amplifies the z, y and x outputs to 0 / 5 V and shows the value of every direction in a VUmeter. The circuit was tested and it was demonstrated that with only two Wheatstone bridges, it is possible to detect the three directions of the acceleration.

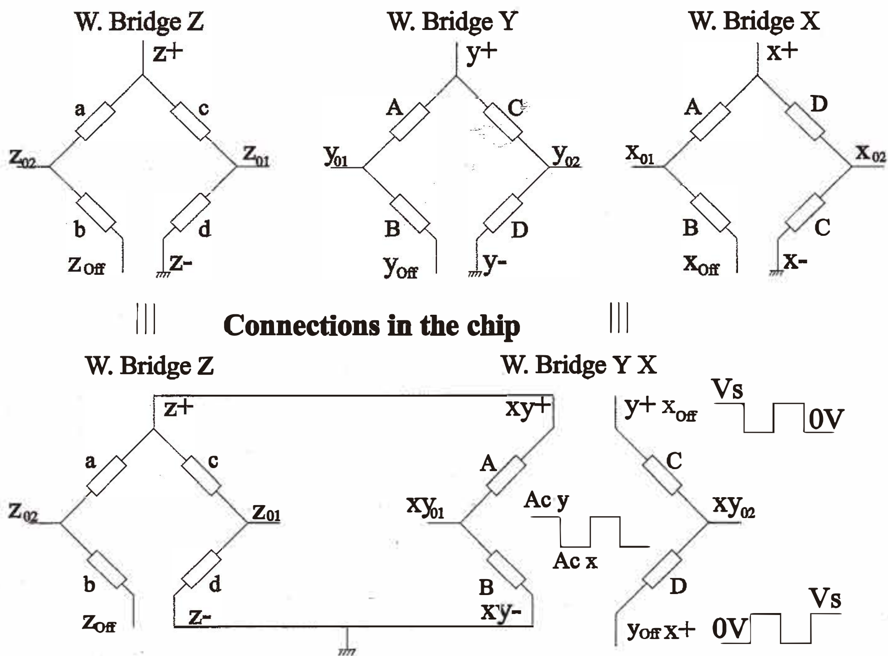

Fig. 7. Theoretical configurations of the eight piezoresistors and connections in the chip.

4. Fabrication

The fabrication process is based on bond and etch back silicon on insulator (BESOI) wafers. The technology is a combination between bulk and surface micromachining.[21] As a consequence it is very simple, and the thickness of the beams is well controlled by the thickness of the silicon over the buried silicon oxide layer. The thickness of the top silicon layer is 15 μm. The anisotropic etching stops automatically at the buried silicon oxide layer. Therefore, the electrochemical etch stop technique is not used, which means that the process is simplified. For example, neither implantation to define the n-well to stop the etch nor the difficult connections used in the electrochemical etch stop are necessary.

The process flow is explained next. After the implantation of the piezoresistors, the opening of the contacts and metallization, the wafers are anisotropically etched in order to define 3D masses, Fig. 8(a). The anisotropic etching stops at the 2 μm buried silicon oxide layer. The buried oxide is laterally etched 50 μm as a sacrificial layer, Fig. 8(b). The length of the lateral etch is controlled by time. This lateral etch allows the fabrication of an overrange protection system without any additional photolithographic step or process. The wafers are then dry etched by RIE in order to define the beams, Fig. 8(c).

The overrange protection system is similar to the LUCAS NOVASENSORS (NAH series). In the process presented in this paper, the maximum displacement of the masses is defined by the thickness of the buried oxide layer, 2 μm. In Fig. 8(d), small salients from the frame limit up movement of the mass, and in Fig. 8(e), small salients from the mass limit its down movement.

Finally, the silicon wafer is anodically bonded to the glass wafer with small cavities. The required damping can be achieved by the control of the gap between the masses of the accelerometer and the glass below the masses and the control of the gap and area of the salients that form the overrange protection system.

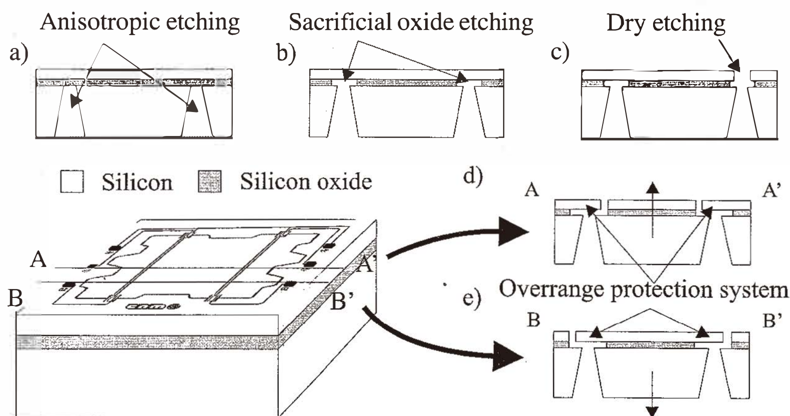

Fig. 8. Fabrication process: (a) anisotropic etching, (b) buried oxide sacrificial etching, (c) dry etching, (d) and (e) overrange protection system.

5. Results

The fabricated devices have been statically characterized by turning them in the gravitational field (Fig. 9). The accelerometer is placed on a disk that can be turned in steps of 10 degrees. In this setup, the acceleration applied to the accelerometer is the gravity acceleration by the cosine of the turned angle, θ. Therefore, the range of the applied acceleration is between 1 g to –1 g. The accelerometer is mounted with appropriate orientation to measure each of the three directions with the appropriate Wheatstone bridge. The outputs of Wheatstone bridges Z , Y and X versus the inclination of the device, when it is turning in the gravitational field, are shown in Fig. 10(a). The same outputs as a function of the applied acceleration are plotted in Fig. 10(b). The experimental output is linear with acceleration.

The sensitivities of the device versus the three components of acceleration and their nonlinearity are shown in Table 4. Note that the sensitivities in the Table 4 are in mV/(V·g) and they must be multiplied by the applied voltage, 5 V, to compare with the Fig. 10. As it is shown in Table 2 and Table 4, the experimental sensitivities are in good agreement with those simulated by ANSYS; except in the case of z direction because in the FEM results a point piezoresistor was considered. It was not considered that the stress was different along the whole piezoresistor. The nonlinearity of the outputs is very low, below 0.6%FS. The cross-sensitivities are lower than 2% for the Z and Y Wheatstone bridges and 8% for the X Wheatstone bridge. The latter is higher than expected. The FEM simulations show that the stress induced in the external beams, where the piezoresistors of the X Wheatstone bridge are situated, when an x acceleration is applied to the accelerometer is 8 times lower than the stress induced by a z acceleration. The change in these piezoresistors is 8 times higher in

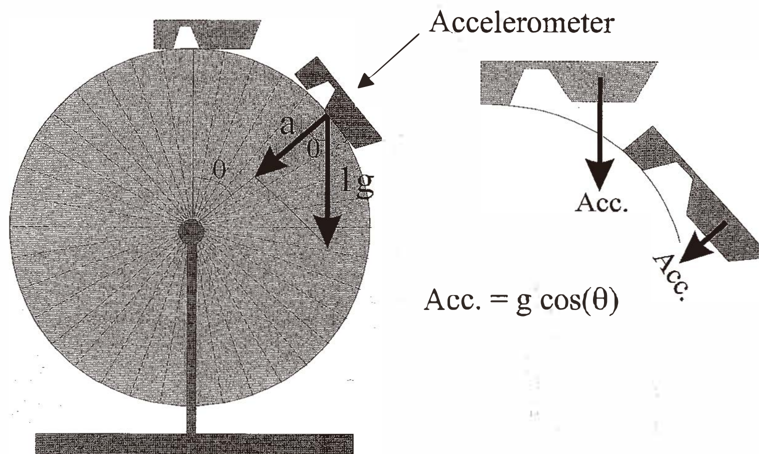

Fig. 9. Setup for the static characterization of the accelerometer.

a)

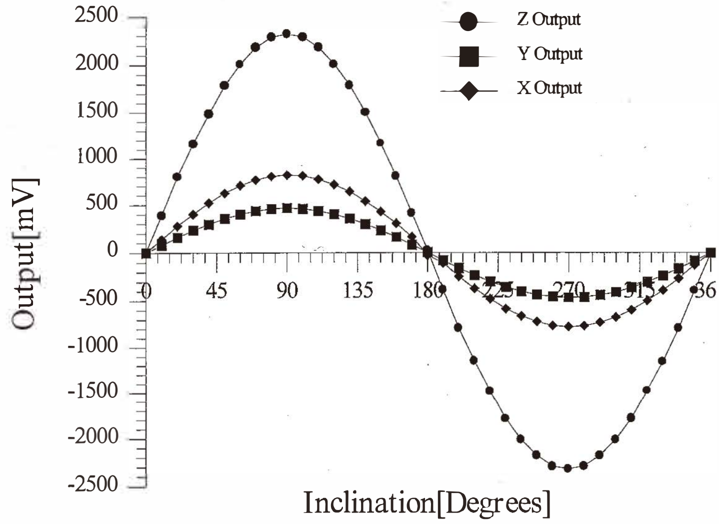

b)

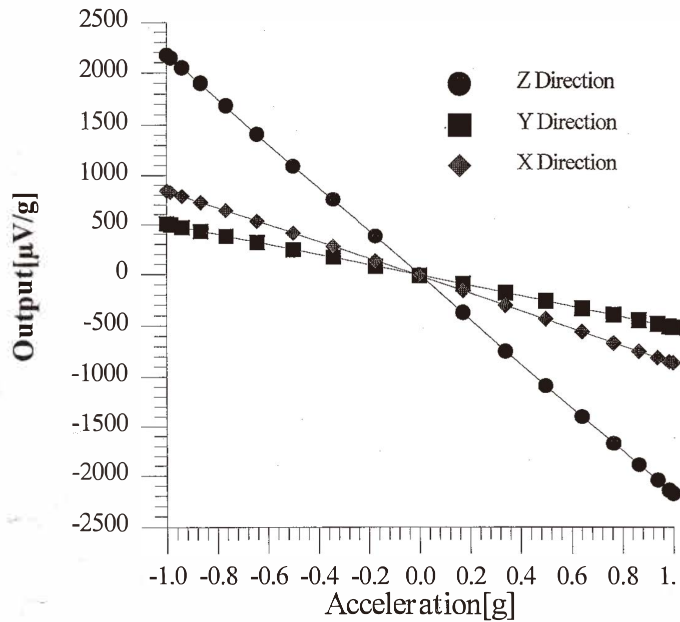

Fig. 10. (a) Output of the devices turned in the gravitational field in the three directions. (b) Output of the devices versus the acceleration in the three directions.

Table 4
Experimental sensitivities and nonlinearities in the three components of the acceleration vector (range: –1 g to 1 g).

	W. bridge X	W. bridge Y	W. bridge Z
Sensitivity [mV/(V·g)]	0.160	0.0926	0.464
Nonlinearity [%FS]	0.52	0.58	0.32

the case of a z acceleration, but the changes of all the piezoresistors have the same sign. Unfortunately, small differences in the piezoresistors are 8 times more important and they can induce a higher value of the cross-sensitivity (8%). This value can be reduced in a new prototype by improving the design, reducing the effect of the z acceleration on the external beams by changing the dimension.

The devices were dynamically characterized on a vibration table. The damping of the device was not optimized, so the bandwidth of the device is limited by its natural frequency, 715 Hz. The nonlinearity of the structures is limited by the overrange protection system and it is lower than 1% in the range ±2 g.

6. Conclusions

A new piezoresistive triaxial accelerometer with theoretically null cross-sensitivity has been designed and fabricated. The structure is similar to a Twin-mass design and consists of two twin masses joined together by two beams and joined to the frame by four external beams. The external beams parallel to the mass reduce the effects of the stresses produced by the package of the devices. The new design presents a higher sensitivity for the z direction than in the case of the Twin-mass design. The increment in the sensitivity of the device is larger than the reduction of its natural frequency so the figure of merit of the new structure is larger than in the case of the standard Twin-mass structure. The introduction of a second central beam reduces more than 20 times the yaw of the twin masses. The number of Wheatstone bridges has been reduced from three to two in order to avoid a large number of metal lines over the beams and therefore, to reduce the level of stresses due to these metal lines on the beams. We have developed a circuit that connected to the triaxial accelerometer shows the outputs of the three directions of the acceleration. The circuit was tested and showed a good performance.

The devices have been fabricated using BESOI wafers. The technology is a combination of bulk and surface micromachining allowing easy fabrication of complex structures. The devices have been characterized and the experimental results agree with the FEM ones. The sensitivity of the devices is high compared with other proposed triaxial accelerometers. The nonlinearity of the devices is lower than 0.6% and the cross-sensitivities are lower than 2% for the z and y directions but 8% for the x direction.

References

1 W. Kuehnel and S. Sherman: Sensors & Actuators A **45** (1994) 7.
2 P. W. Barth, F. Pourahmadi, R. Mayer, J. Poydock and K. Petersen: Technical Digest IEEE, Solid-state Sensor and Actuator Workshop (Hilton Heads Island, South Carolina, 1988) p. 35.
3 A. T. M. Willemsen, C. Frigo and H. B. K. Boom: IEEE Transactions on Biomedical Engineering, vol.38, no.12, December (1991) p. 1186.
4 G. I. Andersson: Transducers' 95-Eurosensors IX (Stockholm, Sweden, 1995) p. 558.
5 T. Mineta, S. Kobayashi, Y. Watanabe, S. Kanauchi, I. Nakagawa, E. Suganuma and M. Esashi: Transducers' 95-Eurosensors IX (Stockholm, Sweden, 1995) p. 554.
6 P. Scheeper, J. O. Gullov and L. M. Kofoed: Journal Micromechanical Microengineering **6** (1996) 131.
7 J. C. Lötters, W. Olthius, P. H. Veltink and P. Bergveld: Eurosensors X (Leuven, Belgium, 1996) p. 441.
8 H. Takao, Y. Matsumoto, H. Seo, M. Ishida and T. Nakamura: Sensors & Actuators A **55** (1996) 91.
9 K. Kwon and S. Park: Transducers' 97 Vol. 2 (Chicago, USA, 1997) p. 1221.
10 M. A. Lemkin, B. E. Boser, D. Auslander and J. H. Smith: Transducers' 97 Vol. 2 (Chicago, USA, 1997) p. 1185.
11 J. C. Lötters, W. Olthuis, P. H. Veltink and P. Bergveld: Transducers' 97 (Chicago, USA, 1997) p. 1177.
12 H. Takao, Y. Matsumoto and M. Ishida: Transducers' 97 (Chicago, USA, 1997) p. 1173.
13 C. V. C. Bouten, K. T. M. Koekkoek, M. Verduin, R. Kodde and D. Janssen: IEEE Transactions on Biomedical Engineering, Vol. 44, No. 3 (1997) p. 136.
14 R. Puers, A. Montano and S. Reyntjens: Eurosensors XI (Warsaw, Poland, 1997) p. 755.
15 Y. Kanda: Sensors & Actuators A **28** (1991) 83.
16 T. Tschan, N. de Rooij, A. Cezinge, S. Ansermet and J. Berthoud.: Sensors & Actuators A **25-27** (1991) 605.
17 S. Shen, J. Chen and M. Bao: Sensors & Actuators A **34** (1992) 101.
18 Chr. Burrer, J. Esteve, J. A. Plaza, M. Bao, O. Ruiz and J. Samitier: Tranducers' 93 (1993) p. 840.
19 H. Chen, M. Bao, H. Zhu and S. Shen: Sensors & Actuators A **63** (1997) 19.
20 J. A. Plaza, H. Hong, J. Esteve and E. Lora-Tamayo, Sensors and Actuators A **66** (1998) 105.
21 J. A.Plaza and J. Esteve: Sensors & Actuators A **68** (1998) 299.